ELSEVIER

Chemical Engineering Journal 107 (2005) 97–102

Chemical Engineering Journal

www.elsevier.com/locate/cej

# Studies on the kinetics of carbon dioxide absorption with immobilised amines (IA)

X. Zhang*, S. Schubert, M. Gruenewald, D.W. Agar

*Department of Biochemical and Chemical Engineering, University of Dortmund, Emil-Figge-Str. 66, D-44227 Dortmund, Germany*

---

## Abstract

An interesting innovative concept for the removal of $CO_2$ from sour gas using immobilised amines (IA) in the $CO_2$ absorption process with methyldiethanolamine (MDEA) has been evaluated in our previous work [2]. The positive effect of IA on the absorption behaviour has been demonstrated by means of preliminary batch experiments in an aerated stirred tank reactor. In order to identify the rate-limiting steps in the three-phase system, experiments with a liquid medium in a fixed-bed reactor have been carried out to establish the absorption kinetics of dissolved $CO_2$ onto IA and the desorption (regeneration) kinetics of $CO_2$-loaded IA with MDEA solution. The breakthrough profiles of $CO_2$ at the outlet of the reactor are measured using a newly developed analytical method. Based on the experimentally determined adsorption and packing parameters, a mathematical model has been developed to describe the experiments and found to yield an accurate prediction of the dynamic $CO_2$ concentration profiles. It could be shown experimentally that the adsorption rate of dissolved $CO_2$ with IA ($k_{\text{liquid–solid}} = 1.54 \times 10^{-7}$ m/s, 298 K) and the desorption rate of $CO_2$-loaded IA ($k_{\text{solid–liquid}} = 5.64 \times 10^{-8}$ m/s, 298 K) are the same order of magnitude and both constitute rate-limiting processes. On the basis of observations and results, two possible mechanisms for this novel three-phase gas–liquid–solid system are proposed and compared with one another.

*Keywords:* Kinetics; Absorption; Desorption; Carbon dioxide; Immobilised amines

---

## 1. Introduction

Blends of primary or secondary amines with tertiary amines, such as MDEA, are frequently used for the removal of $CO_2$ from gas mixtures [1]. These 'activated' amine solutions are advantageous, since they combine the high absorptive capacity of the tertiary amines with the high absorption rates achievable with primary or secondary amines. However, the acceleration of $CO_2$ absorption via the rapid formation of carbamates with primary or secondary amines is usually only required locally within the absorption column. Inside other parts of the absorption process, homogeneous activating additives can give rise to undesirable side-effects, such as increased corrosion or higher energy demands for regeneration. It would thus seem to be preferable to immobilise the activators on a solid carrier, which would ideally also serve as a packing material, within the absorption column. In this way, the activators could be localised in those parts of the absorption process where they are needed and excluded elsewhere.

The positive effect of IA on the absorption behaviour was demonstrated by means of preliminary batch experiments in an aerated stirred tank reactor [2]. In these experiments, an adsorber resin functionalised with benzyl amine (BA) groups (Lewatit VP OC 1065, Bayer AG) was chosen as the IA material. The resin particles are spherical with a diameter of 0.5–1 mm and have a density of 1.092 kg/m$^3$. The concentration of BA groups was determined by titration with 0.1 M HCl to be 0.33 mol/l Lewatit. As discussed in a previous paper [2], IA also provide a similar enhancement of the absorption of $CO_2$ into an aqueous MDEA solution as an equivalent quantity of homogeneous activator (e.g. diethanolamine). Further experiments on the regeneration process have demonstrated that $CO_2$-loaded IA can be regenerated with MDEA solution (0.5 M) and subsequently exhibit the same absorption behaviour as the fresh material. Considerable mass transfer resistance was found in further experiments with a bubble column reactor [2].

---

* Corresponding author. Fax: +49 231 755 2698.
*E-mail address:* zhangx@bci.uni-dortmund.de (X. Zhang).

1385-8947/$ – see front matter © 2004 Elsevier B.V. All rights reserved.
doi:10.1016/j.cej.2004.12.015

**Nomenclature**

| | |
|---|---|
| $a$ | specific area of packed bed ($m^{-1}$) |
| $C_L$ | liquid phase concentration of $CO_2$ ($mol/m^3$) |
| $d_b$ | fixed-bed diameter (m) |
| $d_p$ | particle diameter (m) |
| $D_{ax}$ | axial dispersion coefficient ($m^2/s$) |
| $k$ | mass transfer coefficient (m/s) |
| $k_{eff}$ | LDF mass transfer coefficient ($s^{-1}$) |
| $k_L$ | Langmuir model constant ($m^3/mol$) |
| $q$ | solid phase concentration (mol/kg) |
| $q_{eq}$ | equilibrium solid phase concentration (mol/kg) |
| $q_{max}$ | Langmuir model constant (mol/kg) |
| $t$ | time (s) |
| $u$ | superficial velocity (m/s) |
| $V_b$ | volume of packed bed ($m^3$) |
| *Greek letters* | |
| $\varepsilon_b$ | total voidage of the adsorbent bed |
| $\varepsilon_{ext}$ | external voidage of the adsorbent bed |
| $\varepsilon_{int}$ | pellet voidage |
| $\rho_b$ | bulk density of the adsorbent bed ($kg/m^3$) |
| $\rho_p$ | density of pellet ($kg/m^3$) |
| $\tau$ | mean residence time (s) |

In order to quantify the various mass transfer and reaction steps occurring in the three-phase system and to identify the rate-limiting steps, additional experiments were carried out with gas in a fixed-bed column, in a gas–liquid suspension double-stirred cell reactor and with liquid medium in a fixed-bed column. The objective of this paper is to present kinetic measurements for the adsorption of dissolved $CO_2$ on IA and for the desorption of $CO_2$-loaded IA with MDEA with the liquid medium fixed-bed column. The experiments using gas with a fixed-bed column and the gas–liquid suspension double-stirred cell reactor will be published in detail elsewhere. By way of a theoretical background for the kinetic experiments presented, two possible mechanisms for the three-phase system based on the measured kinetics are suggested and compared with one another in the final section. For the simulation of the experiments, a simple linear-driving-force mathematical model has been developed and found to give an accurate description of the $CO_2$ breakthrough profiles at the reactor exit.

## 2. Mechanisms

For the conventional $CO_2$ absorbing solutions such as monoethanolamine (MEA), diethanolamine (DEA), MDEA etc., well-established reaction mechanisms are available [3,4]. The reaction between $CO_2$ and primary or secondary alkanolamine takes place according to the zwitterion scheme originally proposed by Danckwerts [3], i.e.

$$CO_2 + R_1R_2NH \leftrightarrow R_1R_2N^+HCOO^- \quad (1)$$

$$R_1R_2N^+HCOO^- + B \leftrightarrow R_1R_2NCOO^- + BH^+ \quad (2)$$

The subsequent reaction to the carbamate, takes place via the reaction of the zwitterion with a base B.

Tertiary alknolamines do not react with $CO_2$ directly. The following mechanism has been proposed by Donaldson and Nguyen [4]:

$$CO_2 + R_1R_2R_3N + H_2O \leftrightarrow R_1R_2R_3NH^+ + HCO_3{}^- \quad (3)$$

In this scheme, the tertiary amine acts as a basic catalyst for the reaction between $CO_2$ and water.

Based on the above mechanisms for the reaction between $CO_2$ and alknolamines, two possible mechanisms are suggested for the novel three-phase $CO_2$ absorption system with primary or secondary IA and MDEA. In the first mechanism (see Fig. 1(a)), $CO_2$ from the gas phase, dissolves in the liquid phase (gas–liquid mass transfer). The formation of carbamate then takes place as a kind of chemical adsorption process through the reaction of dissolved $CO_2$ with the IA (liquid–solid 'adsorption'), which would be continuously regenerated 'in situ' by the hydrolysis reaction between the aqueous MDEA solution in the liquid phase flowing over

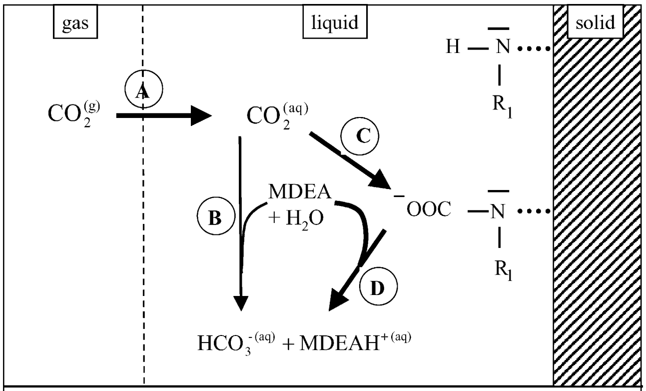

(a) gas-liquid-solid-liquid mechanism

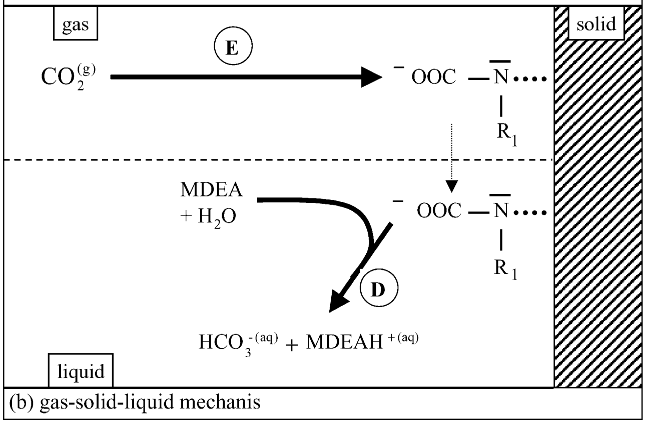

(b) gas-solid-liquid mechanis

Fig. 1. Proposed mechanisms for the three-phase system. A: gas–liquid mass transfer; B: liquid phase reaction; C: liquid–solid 'adsorption' (formation of carbamate); D: solid–liquid 'desorption' (regeneration of immobilised amine) and E: gas–solid 'adsorption' (formation of carbamate).

the IA and the carbamate releasing bicarbonate into the solution (solid–liquid ‘desorption’). In the second mechanism (see Fig. 1(b)), the gas phase first contacts with the solid phase directly and the carbon dioxide adsorbs on the surface of the solid forming carbamate (gas–solid ‘adsorption’). The gas phase is then replaced by the liquid phase with the solid–liquid ‘desorption’ taking place as in the first mechanism.

There are four individual steps in the mechanisms described, i.e. the gas–liquid mass transfer, the gas–solid ‘adsorption’, the liquid–solid ‘adsorption’ and the solid–liquid ‘desorption’. To identify the rate-limiting step in the three-phase system, it is necessary to measure the kinetics of these four steps separately. The kinetics for gas–liquid mass transfer ($k_{\text{gas–liquid}} = 3.6 \times 10^{-5}$ m/s, 298 K) has been determined in a gas–liquid double-stirred cell reactor, while the kinetics of gas–solid adsorption (quasi-instantaneous) were measured with gas flow in a fixed-bed column. These experiments will be presented in other papers.

## 3. Model and simulation

An unsteady-state mathematical model has been developed to describe the process of adsorption of $CO_2$ and desorption on primary or secondary IA, which describes the equipment parameters, the absorption and desorption kinetics and the breakthrough curves at the outlet of the packed bed.

The main model assumptions are summarised as follows: an isothermal, isobaric operation, ‘adsorption’ equilibrium described by a single-site Langmuir type model, adsorption kinetics described by a linear-driving-force model, plug flow with axially dispersion within the adsorbent fixed-bed. Based on the above assumptions, $CO_2$ mass balances for the fixed-bed can be written as:

$$\varepsilon_b \frac{\partial C_L}{\partial t} + \rho_b \frac{\partial q}{\partial t} = D_{ax} \frac{\partial C_L^2}{\partial z^2} - u \frac{\partial (C_L)}{\partial z} \qquad (4)$$

where $\varepsilon_b$ is the total voidage of the adsorbent bed. It is calculated from:

$$\varepsilon_b = \frac{\pi d_b^2 u}{4 V_b} \tau \qquad (5)$$

where the mean residence time $\tau$ is experimentally calculated from a preliminary tracer experiment with 0.1 M NaCl solution, with a conductivity detector being used for the detection of the output concentration. Axial dispersion coefficient $D_{ax}$ is evaluated by the simulation of the concentration–time profile in this experiment with the above model.

The single-site Langmuir model can be written as

$$q_{eq} = q_{max} \frac{k_L c_L}{1 + k_L c_L} \qquad (6)$$

where the model parameter $k_L$ and $q_{max}$ are evaluated from the adsorption data derived from experiments with different $CO_2$-concentrations.

As mentioned above, the linear-driving-force model, used in this research to describe the adsorption and desorption of dissolved $CO_2$ on IA, can be written as:

$$\frac{\partial q}{\partial t} = k_{eff} a (q_{eq} - q) \qquad (7)$$

where $k_{eff}$ is the effective mass transfer coefficient, which is determined from the simulation of the concentration–time profiles for adsorption and desorption independently. The specific surface area a of the fixed-bed is given by:

$$a = \frac{6}{d_p}(1 - \varepsilon_{ext}) \qquad (8)$$

where $d_p$ is the pellet diameter and $\varepsilon_{ext}$ is the external voidage of the bed calculated from:

$$\varepsilon_{ext} = \frac{\varepsilon_b - \varepsilon_{int}}{1 - \varepsilon_{int}} \qquad (9)$$

where $\varepsilon_{int}$ denotes the internal voidage of the particles.

The back mixing effects in the tubing and pump before and after the adsorbent fixed-bed are takes into account through a modification of the feed signal for the fixed-bed. The model sensitivity to the mass transfer kinetics is acute.

## 4. Experimental

A fixed-bed reactor with a diameter of 20 mm and height of 110 mm was used for the kinetic measurements of $CO_2$ adsorption (dissolved in water) with the IA and the desorption of $CO_2$-loaded IA with an aqueous MDEA solution (see Fig. 2). It is packed with 34.5 ml Lewatit. Two electric conductivity detectors are employed before and after the fixed-bed for the rapid qualitative detection of $CO_2$-concentration variations. Furthermore, for the quantitative detection of $CO_2$-concentration, samples are collected during the experiment. Due to the difficulty in conserving and analysing the $CO_2$–water samples collected during the adsorption experiments, a new analytical method has also been developed, which can be described as follows: a 8 ml sample is first taken at the exit of the reactor and 1 ml 0.5 M NaOH added (to ‘fix’ $CO_2$ in the aqueous phase). Five hundred microlitres of the resultant sample is then injected into a flask containing concentrated sulphuric acid. The temperature of the bottle is maintained at 85 °C to ensure instant release of $CO_2$ from the liquid phase through the interaction between the injected sample and sulphuric acid. The $CO_2$ is then swept away by constant helium gas flush (50 ml/min) through a cooler (5 °C) to a TCD (thermal conductivity detector). The mass of $CO_2$ in the sample is calculated from the area of $CO_2$-peak detected by the TCD. This method is calibrated using $Na_2CO_3$ solution of various concentrations. The $CO_2$–MDEA–water samples collected in the desorption process are analysed directly using a capillary GC, due to the extensive oxidation of MDEA in the samples with concentrated sulphuric acid.

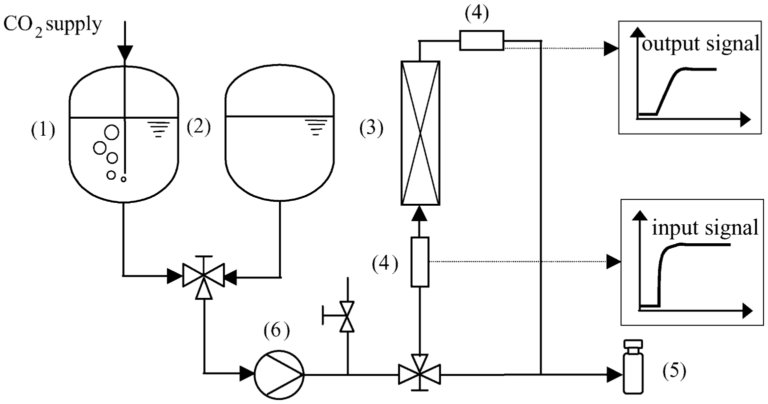

Fig. 2. Schematic diagram of the measurement equipment. (1) $CO_2$ saturated water feed tank; (2) MDEA feed tank; (3) fixed-bed reactor; (4) electrical conductivity detector; (5) sample collector and (6) pump.

The temperature of the $CO_2$ saturated water feed tank is maintained at 20, 25 and 30 °C, respectively, for different experiments. To ensure that the dissolved-$CO_2$ does not gas out from the water either during its passage through the tubing or the adsorption in the fixed-bed, the temperature of the bed is kept 5 °C lower than that of the feed tank.

As the first preparatory step in a typical adsorption experiment, $CO_2$ is bubbled into doubly distilled water in the feed tank for 4 h in order to saturate the water. The water with dissolved $CO_2$ is then fed to the fixed-bed column at different constant flow rates and the adsorption kinetics measured. An electrical conductivity detector is used to record the change of $CO_2$ concentration at the exit of the reactor. Samples are simultaneously collected during the course of the experiment.

For the determination of the regeneration parameters, aqueous MDEA solutions with various concentrations are fed into the $CO_2$-loaded fixed-bed column. Conductivity measurements and samples are also taken as described above. A summary of design and operating parameters used in the experiments and simulations is given in Table 1.

## 5. Results and discussion

To start with, the input and output concentration–time profiles with tracer solution (0.1 M NaCl) were measured and simulated (Fig. 3). Based on the simulation, the axial dispersion coefficient $D_{ax}$ was determined as $7.858 \times 10^{-7}\ m^2/s$ at 15 °C and the bed porosity $\varepsilon_b$, as 0.6144.

Table 1
Packed bed and operation parameters

| | |
|---|---|
| Packed bed | |
| Length of packed zone | 110 mm |
| Diameter of packed zone | 20 mm |
| Particle diameter | 0.5–1 mm |
| Bed voidage | 0.6144 |
| Particle voidage | 0.232 |
| Particle pore volume | $0.27\ m^3/kg$ |
| Bulk density of the adsorbent bed | $540\ kg/m^3$ |
| Particle density | $1118\ kg/m^3$ |
| Operation parameter | |
| Temperature of the bed | 15, 20, 25 °C |
| Temperature of the water tank | 20, 25, 30 °C |

For the reaction between $CO_2$ and IA, due to its similarity with adsorption and desorption process, a isotherm adsorption model (e.g. a single-site Langmuir isotherm model) is used to simulate the isotherm data of this reaction and found that the model fit the experimental data very good (see Fig. 4). A dual-site Langmuir model is ruled out in this work, concerning the simplification of the simulation.

The loading of $CO_2$ on IA for experiments with various $CO_2$-concentration are calculated from the input and adsorption concentration–time profiles (Figs. 3 and 5). The adsorption data were then fitted using the single-site Langmuir model (see Fig. 4) and the adsorption parameters deter-

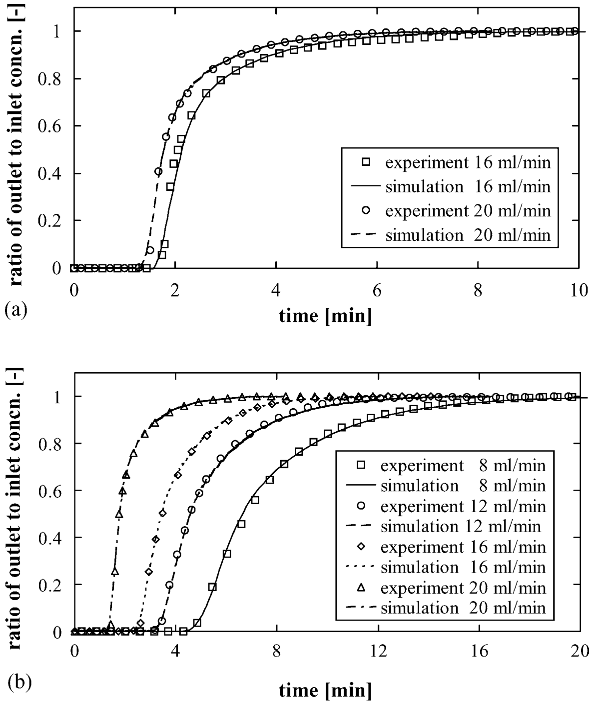

Fig. 3. Measured and simulated input signal (a) and tracer output signal (b).

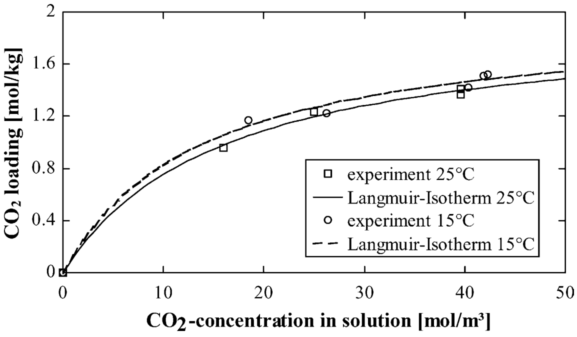

Fig. 4. The simulation of calculated adsorption data with a Langmuir isotherm model.

mined are given in Table 2. With the packing and adsorption parameters found, the linear-driving-force model is implemented with the adsorption and desorption being simulated separately.

Examples of measured and simulated concentration–time profiles are illustrated in Figs. 5 and 6 for the adsorption and desorption steps, respectively. Fig. 5 shows that the model accurately describes the adsorption at various $CO_2$-concentrations, flow rates and temperatures. The $CO_2$-concentration has a significant influence on the adsorption rate (Fig. 5(a)), flow rate however exerts little influence (Fig. 5(b)). From such data, effective mass transfer kinetics $k_{eff}$ could be estimated at 15 and 25 °C (see Table 2). It should be noted that mass transfer rate at 25 °C is larger than that at 15 °C, i.e. the mass transfer kinetics of adsorption increases with the rising temperature.

For desorption of the $CO_2$-loaded IA, it can be seen that the temperature and flow rate both have positive influence on the process in Fig. 6(a) and (b). Fig. 7 shows the simulation of desorption at 25 °C with 0.5 M MDEA. The model is sensitive to the effective mass transfer rate of desorption. The desorption mass transfer kinetics at 25 °C were estimated (Table 3).

Finally, all of the mass transfer coefficients for the above-mentioned four steps of the gas–liquid–solid system are summarised in Table 3. The data shows that the gas–solid adsorption step is the fastest step in the process. The liquid–solid adsorption and solid–liquid desorption steps are rate-limiting steps (exhibiting the same order of magnitude). Both would retard the overall mass transfer. Considering the fast gas–solid adsorption step, the second gas–solid–liquid mechanism would be faster than the first gas–liquid–solid–liquid one. Thus, it is desirable to suppress the first mechanism and encourage the second one in the absorber.

Table 2
Calculated adsorption parameters

| Temperature (K) | $q_{max}$ (mol/kg) | $k_L$ ($m^3$/mol) | $k_{eff}a$ ($s^{-1}$) | $k_{eff}$ (m/s) |
|---|---|---|---|---|
| 288 | 1.969 | 0.0721 | $4.9 \times 10^{-4}$ | $1.21 \times 10^{-7}$ |
| 298 | 1.970 | 0.0632 | $6.2 \times 10^{-4}$ | $1.54 \times 10^{-7}$ |

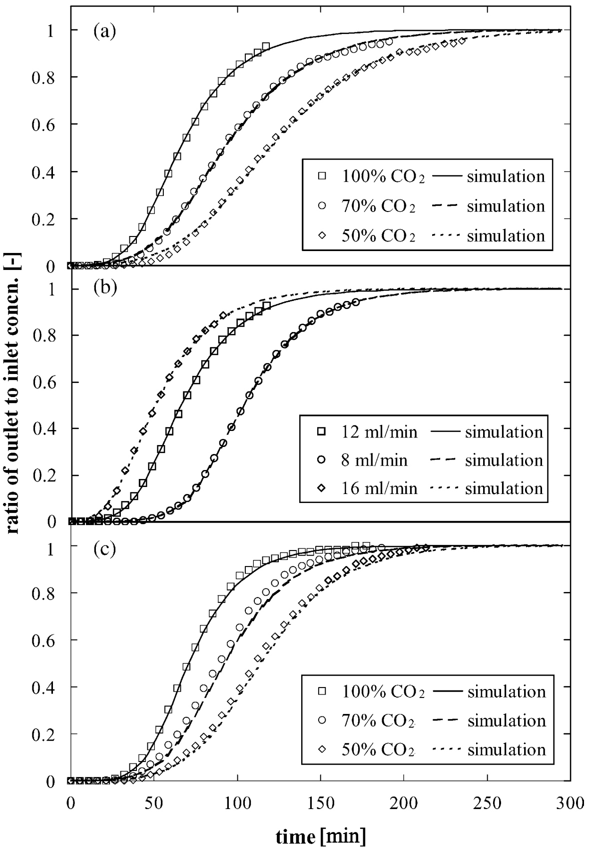

Fig. 5. Measured and simulated adsorption profiles: (a) and (b) 288 K and (c) 298 K.

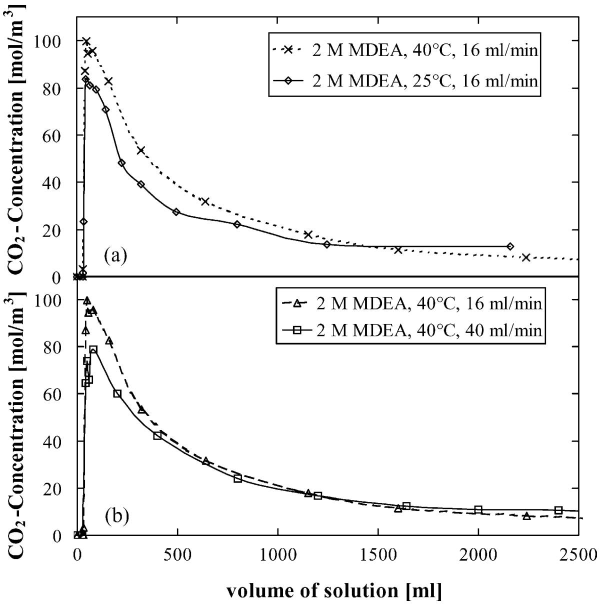

Fig. 6. Measured desorption profiles: (a) influence of temperature and (b) influence of flow rate.

Table 3
Comparison of mass transfer kinetics for different steps at 298 K

| | Mass transfer process | $k_{\mathrm{eff}}$ ($10^{-8}$ m/s) | $k_{\mathrm{eff}}a$ ($10^{-4}$ s$^{-1}$) | Assessment |
|---|---|---|---|---|
| Gas–liquid | Absorption | 3600 | 1458 | Slow |
| Gas–solid | Adsorption | Instantaneous | Instantaneous | Instantaneous |
| Liquid–solid | Adsorption | 15.4 | 6.2 | Rate-limiting |
| Solid–liquid | Desorption/regeneration | 5.6 | 2.3 | Rate-limiting |

Furthermore, as the rate-limiting steps, the liquid–solid adsorption and solid–liquid desorption steps both include two sub-steps, i.e. formation or hydrolysis of carbamate and mass transfer of $CO_2$ or $HCO_3^{-1}$ through the liquid film around the particle surface, kinetics of which can be assumed to be equal to that of $CO_2$ in MDEA solution ($k = 5.656 \times 10^{-5}$ m/s, 313 K) [5]. Both sub-steps could contribute to the mass transfer residence of the above rate-limiting steps.

As a consequence of the above and to circumvent the limitations on mass transfer imposed by the presence of a liquid film on the surface of the IA, a periodic operation of the fixed-bed with alternating liquid and gas cycles is being investigated. In the periodic fixed-bed operation, the solid phase is contacted alternately with gas and liquid. $CO_2$ would thus first be adsorbed on the solid during the gas–solid contact phase and then regenerated 'in situ' again during the subsequent liquid–solid contact interval. This process would be recycled in the fixed-bed as a 'micro-cycle' and $CO_2$ from sour gas be separated continuously.

Sterically hindered amines [6] would be considered as a possible solution to accelerate the reaction rate of regeneration through weakening the bond strength of carbamate by sterically hindrance.

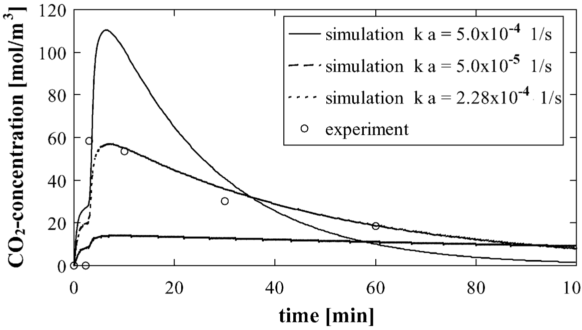

Fig. 7. Measured and simulated desorption profiles at 25 °C with 0.5 M MDEA.

## 6. Conclusions

Experiments to determine the mass transfer kinetics of dissolved $CO_2$ on IA have been carried out. Based on the experimentally determined adsorption and packing parameters, a mathematical model has been developed to describe the experiments and found to give an accurate description of the dynamic concentration profiles of $CO_2$ at the reactor outlet. The effective mass transfer kinetics between liquid and solid have been estimated using the model developed. It could be shown by the experiments in liquid flow fixed-bed that the adsorption rate of dissolved $CO_2$ with immobilised amines is slow and the regeneration kinetics of $CO_2$-loaded IA is the same order of magnitude as that of absorption. Both steps are thus rate-limiting. The existence of considerable mass transfer resistance in liquid film is configured, which might be circumvented in a periodically operated fixed-bed reactor.

## Acknowledgements

The authors would like to thank Max-Buchner-Forschungsstiftung for their support of this work, and Mr. M. Schlüter and J. Gies for their experimental assistance.

## References

[1] A.L. Kohl, R.B. Nielsen, Gas Purification, Gulf Publishing Company, Houston, 1997.

[2] S. Schubert, M. Grünewald, D.W. Agar, Chem. Eng. Sci. 56 (2001) 6211–6216.

[3] P.V. Danckwerts, The reaction of carbon dioxide ethanolamines, Chem. Eng. Sci. 34 (1979) 443–446.

[4] T.L. Donaldson, Y.N. Nguyen, Carbon dioxide reaction kinetics and transport in aqueous amine membranes, Ind. Eng. Chem. Fundam. 19 (1980) 260–266.

[5] E.B. Rinker, S.S. Ashour, O.C. Sandall, Kinetics and modelling of carbon dioxide absorption into aqueous solutions of *N*-methyldiethanolamine, Chem. Eng. Sci. 50 (1995) 755–768.

[6] A.M. Goldstein, Commercialization of a new gas treating agent., in: Paper Presented at Petroenergy'83 Conference, Houston, TX, September 14, 1983.